AGU ADVANCING EARTH AND SPACE SCIENCE

Water Resources Research

RESEARCH ARTICLE
10.1029/2021WR029638

Key Points:

- Variations in mean annual ET_N/ET_D ratio (5.1%–11.7%) across the sites were mostly determined by the spatial variability in ET_D
- ET_D and ET_N responded differently to climatic drivers from half-hourly to annual scales, which also depended on ecosystems types
- At site levels, leading controls were Rn for half-hourly ET_D, leaf area index (LAI), and soil water content (SWC) for daily to annual ET_D, and SWC for half-hourly to annual ET_N

Supporting Information:

Supporting Information may be found in the online version of this article.

Correspondence to:

T. Wang,
tiejun.wang@tju.edu.cn

Citation:

Han, Q., Wang, T., Wang, L., Smettem, K., Mai, M., & Chen, X. (2021). Comparison of nighttime with daytime evapotranspiration responses to environmental controls across temporal scales along a climate gradient. *Water Resources Research*, *57*, e2021WR029638. https://doi.org/10.1029/2021WR029638

Received 17 JAN 2021
Accepted 24 JUN 2021

Comparison of Nighttime With Daytime Evapotranspiration Responses to Environmental Controls Across Temporal Scales Along a Climate Gradient

Qiong Han[1], Tiejun Wang[1,2,3], Lichun Wang[1,2,3], Keith Smettem[4], Mai Mai[1], and Xi Chen[1,2,3]

[1]School of Earth System Science, Institute of Surface-Earth System Science, Tianjin University, Tianjin, People's Republic of China, [2]Tianjin Key Laboratory of Earth Critical Zone Science and Sustainable Development in Bohai Rim, Tianjin University, Tianjin, People's Republic of China, [3]Critical Zone Observatory of Bohai Coastal Region, Tianjin University, Tianjin, People's Republic of China, [4]Institute of Agriculture, The University of Western Australia, Crawley, WA, Australia

Abstract Understanding daytime (ET_D) and nighttime (ET_N) evapotranspiration is critical for accurately evaluating terrestrial water and carbon cycles. However, unlike ET_D, the factors influencing ET_N remain poorly understood. Here, long-term ET_D and ET_N data from five FLUXNET sites along a climate gradient in Northern Australia were analyzed to compare their responses to environmental drivers at different temporal scales. We found that (a) across the sites, mean annual ET_N/ET_D ($\overline{ET_N}$ / $\overline{ET_D}$) ranged between 5.1% and 11.7%, which was mainly determined by $\overline{ET_D}$ variations. Particularly, vegetation and meteorological variables mostly controlled $\overline{ET_D}$, while $\overline{ET_N}$ was largely related to air temperature and net radiation (Rn) due to lower nighttime atmospheric water demands; (b) At individual sites, ET_D and ET_N exhibited higher correlations with meteorological and vegetation variables at monthly timescales than at annual timescales. Monthly ET_D and ET_N were also strongly coupled, especially under drier climatic conditions. At daily timescales, leaf area index and soil water content (SWC) controlled ET_D with SWC being more important at drier sites; whereas, SWC was the dominant factor controlling ET_N. At half-hourly timescales, the boosted regression tree method quantitively showed that ET_D and ET_N were controlled by Rn and SWC, respectively. Overall, the results showed that ET_N was less responsive to environmental variables, illustrating that ET_D and ET_N responded differently to diverse climate regimes and ecosystems at varying temporal scales. These findings provide a critical evaluation for contrasting ET_D and ET_N interactions in constantly changing environments, which has important implications for ecosystem water balance and land surface processes modeling.

1. Introduction

As one of the key components in terrestrial water cycles, actual evapotranspiration (ET) links water, energy, and carbon cycles via plant physiological activities (Fisher et al., 2017; Katul et al., 2012). Although ET is primarily composed of daytime ET (ET_D), a growing body of observational and modeling evidence suggests that nighttime ET (ET_N) is also important for various ecohydrological and physiological processes from local to global scales (Forster, 2014; Padrón et al., 2020; Whitley et al., 2013). Globally, Padrón et al. (2020) showed that the average ET_N/ET value was about 6.3% when calculated from the FLUXNET2015 data set and 7.9% from simulation results of global models. Moreover, ET_N can exert significant impacts on the estimation of global water and carbon budgets, particularly in arid and semiarid regions (Lombardozzi et al., 2017; Resco De Dios et al., 2015), since the consideration of nighttime water use as indicated by ET_N can noticeably reduce water use efficiency (WUE, defined as the ratio of CO_2 assimilation rate over water vapor loss) (Chaves et al., 2016). At field scales, neglecting ET_N can cause the underestimation of total daily ET and the incomplete closure of energy balance, thus resulting in underestimated water requirements for crops (Skaggs & Irmak, 2011). Therefore, in addition to the role of ET_D, a better understanding of nighttime water loss from terrestrial ecosystems also bears many important implications for hydrological, climatic, and agricultural studies (Agam et al., 2012; Berkelhammer et al., 2013; Wang & Dickinson, 2012).

To accurately evaluate the impacts of ET_D and ET_N on ecohydrological and biogeochemical processes, it is critical to elucidate how they respond to changes in environmental conditions. However, the majority of relevant nighttime studies focused on nighttime transpiration (Tr_N), which is part of ET_N and can account

for up to 69% of total daily transpiration (Tr) for certain equatorial species (Forster, 2014). The mechanism that controls Tr_N is mainly attributed to incomplete stomatal closure at night (Dawson et al., 2007; Duursma et al., 2019), although other regulation mechanisms have also been proposed, such as the circadian regulation of nighttime water use by plants (Resco De Dios et al., 2015). Despite the debate on the underlying regulation mechanisms, a wealth of studies have revealed the complex interactions of Tr_N with surrounding environments (Iritz & Lindroth, 1994; Moore et al., 2008). The spatiotemporal variations in Tr_N have been linked to changes in soil water content (SWC) (Barbeta et al., 2012; O'keefe & Nippert, 2018), vapor pressure deficit (VPD) (Bucci et al., 2004; Tolk et al., 2006), and wind speed (WS) (Karpul & West, 2016). However, inconsistent findings have also been reported. For instance, Tr_N was shown to be positively related to VPD and SWC (Dawson et al., 2007; Moore et al., 2008), while no or negative relationships were also found between Tr_N and VPD (or SWC) (Barbour & Buckley, 2007; Phillips et al., 2010; Resco De Dios et al., 2015). In addition, biotic factors (e.g., plant species and ecosystem type) might also play important roles in determining Tr_N (O'keefe & Nippert, 2018; Zeppel et al., 2014). As a result of the combined influence of biotic and abiotic factors, Tr_N (and thus ET_N) is highly variable among different plant species, ecosystems, and climate regimes (see Table S1 in the supplemental information for details).

Although previous work has focused on Tr_N, it is more relevant from hydrological and water resources management perspectives to quantify ET_N and particularly how it changes with environmental variables. As different components of ET (e.g., Tr, and soil and canopy evaporation) respond to environmental factors differently (Tsuruta et al., 2016), it would be questionable to directly extrapolate the findings obtained from Tr_N studies to understand ET_N behaviors under changing environmental conditions. Similar to Tr_N, ET_N can be affected by a number of biotic and abiotic factors. At field scales, Skaggs and Irmak (2011) showed that ET_N was a function of weather conditions (e.g., VPD, WS, and net radiation-Rn), and the relative influence of these variables further varied with crop growing stages. Using eddy-covariance (EC) records from two forested ecosystems, Novick et al. (2009) observed that ET_N was primarily driven by WS and VPD, and Tr_N was the leading contribution to ET_N. By contrast, based on lysimeter measurements under natural grass covers, Groh et al. (2019) found that ET_N was mainly composed of evaporation and positively correlated with WS. The authors also showed the importance of night dew formation in controlling ET_N at the study sites. In short, the dominant environmental factors controlling ET_N were inconsistent in previous studies and remained poorly understood (Groh et al., 2019; Padrón et al., 2020; Zeppel et al., 2014).

More importantly, previous studies showed that dominant controls on ET_D and ET_N might be different (Barbeta et al., 2012; Karpul & West, 2016; O'keefe & Nippert, 2018), implying that ET_N cannot simply be estimated from ET_D alone and should be investigated separately (Groh et al., 2019; Ogle et al., 2012). For example, Groh et al. (2019) showed that at grassland sites from Germany, Rn and VPD were the dominant controls on ET_D, while ET_N was more strongly influenced by WS. O'keefe and Nippert (2018) argued that daytime and nighttime stomatal conductance should be parameterized separately in land surface models. In addition, the main controls on ET can change across temporal scales. For instance, Scott and Biederman (2019) found that the dominant controls on ET changed from subdaily (weather) to seasonal (SWC) scales in a semi-arid savanna ecosystem, indicating that controlling factors of ET_D and ET_N might also vary with temporal scales. Part of the reason can be attributed to the varying correlations among environmental factors across temporal scales, as stressed by Liu et al. (2020).

For the global study, Padrón et al. (2020) showed that for most FLUXNET sites, there were positive correlations of daily ET_N/ET with local air temperature (T_a), Rn, and SWC at individual sites; however, no clear relationships of mean annual ET_N/ET ($\overline{ET_N}/\overline{ET}$, where overbar denotes mean annual timescales hereinafter) with precipitation ($\overline{P}$) and $\overline{T_a}$ were found across those sites. With regards to biotic factors, the relationship between $\overline{ET_N}/\overline{ET}$ and ecosystem types was also weak across FLUXNET sites (Padrón et al., 2020). As ET is primarily composed of ET_D, the lack of general patterns from the study of Padrón et al. (2020) clearly demonstrated the poor correlation between ET_D and ET_N across different climate regimes and ecosystem types. Based on above discussions, we hypothesize that this could be attributed to the different responses of ET_D and ET_N to diverse climate regimes and ecosystems at varying temporal scales. Elucidation of the interactions of ET with environmental drivers at different timescales is critical for understanding a variety of ecohydrological and land surface processes. For instance, annual and monthly ET processes are related to vegetation phenology and therefore important for estimating terrestrial productivity (Berkelhammer

et al., 2013). At daily and subdaily timescales, ET dynamics involving areas from genetics to physiology would affect plant performance and WUE (Chaves et al., 2016). Thus, the aforementioned studies underscore the necessity of differentiating the mechanistic responses of ET_D and ET_N to influencing factors at different temporal scales, for example, for quantifying and/or modeling ET_D and ET_N purposes.

To test our hypothesis, the spatiotemporal characteristics of ET_D and ET_N as well as their relationships with environmental drivers were analyzed using long-term EC records obtained at five FLUXNET sites along a climate gradient from Northern Australia. Based on data from the Australian Bureau of Meteorology (data available from 1973 to 2015), northern Australia exhibits a strong P gradient along the north-south direction with a monsoonal climate of distinct wet and dry seasons (Beringer et al., 2016). This P gradient aligns with structural and floristic changes in the composition of local vegetation communities (Hutley et al., 2011; Williams et al., 1996), making this region suitable for studying the spatiotemporal variations in ET_D and ET_N and for examining their responses to environmental variables. The responses of ET_D and ET_N to environmental controls along this climate gradient were analyzed from mean annual to half-hourly timescales. In addition, a nonlinear machine learning method, namely the boosted regression tree (BRT), was employed to quantify the relative controls of environmental factors on ET_D and ET_N at half-hourly timescales.

2. Materials and Methods

2.1. Site Description

For the purpose of this study, five sites installed with EC towers were selected (Table 1), which are distributed along the North Australian Tropical Transect (NATT; Figure 1). The NATT spans roughly 900 km, stretching from Darwin (about 12°S) in the mesic north of the Northern Territory to the xeric edge of the Tanami Desert (about 17°S) (Schulze et al., 1998). Along the NATT, $\overline{T_a}$ shows no significant gradient (~26°C across the sites), while $\overline{P}$ decreases noticeably from ~1,800 mm/year in the north to ~200 mm/year in the south (Schulze et al., 1998). There is a pronounced climate seasonality in the study region, with a dry season extending from May to September.

Dominant vegetation communities in the study region tend to be savannas, which are characterized by a patchy woody overstory (mainly evergreen *Eucalyptus* and *Corymbia* tree species) and an understory (mainly C4 grasses) (Whitley et al., 2016). The abundance and height of the overstory eucalypts decrease with declining $\overline{P}$ from north to south, and understory grasses die off immediately at the end of wet seasons (Hutley et al., 2011). In addition, tropical grasslands dominate the intermediate, semi-arid section of the NATT (e.g., at the AU-DaP and AU-Stp sites [Site ID from the FLUXNET]). Soil types range from sand-dominated Kandosols in the north to Vertosols or cracking clays that are more widespread in the south (Australian Soil Classification [Isbell, 2002]). The alternating wet and dry seasons and the redox of metal-rich soils produce duricrusts in soils with varying depths, which ultimately limit vegetation growth (Dilshad et al., 1996; Hutley et al., 2011). Relevant information for each site is summarized in Table 1.

2.2. Data Acquisition

The FLUXNET is a global network equipped with EC towers to measure site-level water, carbon, and energy exchanges between the atmosphere and biosphere (Baldocchi et al., 2001). In this study, half-hourly meteorological and soil data (e.g., latent heat-*LE*, sensible heat-*H*, soil heat flux-*G*, *P*, SWC, T_a, *Rn*, VPD, WS, and friction velocity-u^*) measured at the five FLUXNET sites were retrieved from the FLUXNET 2015 Tier 1 data set (https://fluxnet.org/data/fluxnet2015-dataset/). Here, the data set is briefly discussed, and the detailed descriptions can be found at http://www.ozflux.org.au/and in Beringer et al. (2016). Specifically, a CSAT3 sonic anemometer (Campbell Scientific, Logan, Utah, USA) and a Li-7500 infra-red gas analyzer (LI-COR, Lincoln, Nebraska, USA) are mounted at the top of the EC towers with the height of 23 m, 15 m, 23 m, 15 m, and 4.8 m above the ground at AU-How, AU-DaP, AU-DaS, AU-Dry, and AU-Stp, respectively. The EC towers record wind field (WS and u^*) and H_2O concentrations at 10 Hz or 20 Hz, which are then integrated to half-hourly data. Radiation (NR-Lite, Kipp & Zonen, Delft, Netherlands), and T_a and relative humidity (HMP45AC or HMP45 A, Vaisala, Helsinki, Finland) are measured at the tower top, while P (TB3, HyQuest Solutions, New South Wales, Australia; CS702, Campbell Scientific, Utah, USA) is measured at the ground. Soil variables, including SWC (CS616, Campbell Scientific, Utah, USA) and G (HFT3, Campbell Scientific,

Water Resources Research

10.1029/2021WR029638

Table 1
Information for the Five Study Sites Along the North Australian Tropical Transect

Site ID	year	Latitude (°)	Longitude (°)	Elevation (m)	$\overline{T_a}$(°C/year)	$\overline{P}$(mm/year)	$\overline{ET_p}$ (mm/year)	$\overline{ET_p}/\overline{P}$	Daytime $\overline{Tr}/\overline{ET}$	Soil type	Ecosystem	Species	Canopy height (m)
AU-How	2002–2014	12.49°S	131.15°E	64	26.7	1715.5 (1112.0–2287.4)[a]	1689.5	0.98	0.56	Sandy loam (kandosol)	Savanna	*Eucalyptus miniata* *Eucalyptus tetrodonta*	15
AU-DaP	2008–2013	14.06°S	131.32°E	70	25.5	1402.8 (945.1–1723.9)	1704.2	1.21	0.64	Sandy loam (kandosol)	Grassland	*Chamaecrista rotundifolia* *Digitaria milijiana*	0.3
AU-DaS	2009–2014	14.16°S	131.39°E	110	26.7	1400.1 (1167.7–1599.4)	1851.6	1.32	0.51	Sandy loam (kandosol)	Savanna	*Eucalyptus tetrodonta* *Corymbia latifolia*	16.4
AU-Dry	2009–2014	15.26°S	132.37°E	175	26.9	890.4 (655.1–1396.2)	1843.6	2.07	0.50	Sandy loam (kandosol)	Savanna	*Eucalyptus tetrodonta* *Corymbia terminalis*	12.3
AU-Stp	2009–2014	17.15°S	133.35°E	250	26.1	761.1 (473.6–1135.6)	2146.2	2.82	0.46	Cracking clay (vertisol)	Grassland	*Mitchell Grass*	0.5

[a]The range of annual precipitation during the study period; $\overline{T_a}$: mean annual temperature; $\overline{P}$: mean annual precipitation; $\overline{ET_p}$: mean annual potential evapotranspiration; $\overline{ET_p}/\overline{P}$: mean annual aridity index; Daytime $\overline{Tr}/\overline{ET}$: long-term ratio of transpiration to actual evapotranspiration during the daytime (following the method of Zhou et al., 2016 as described in the supplemental materials).

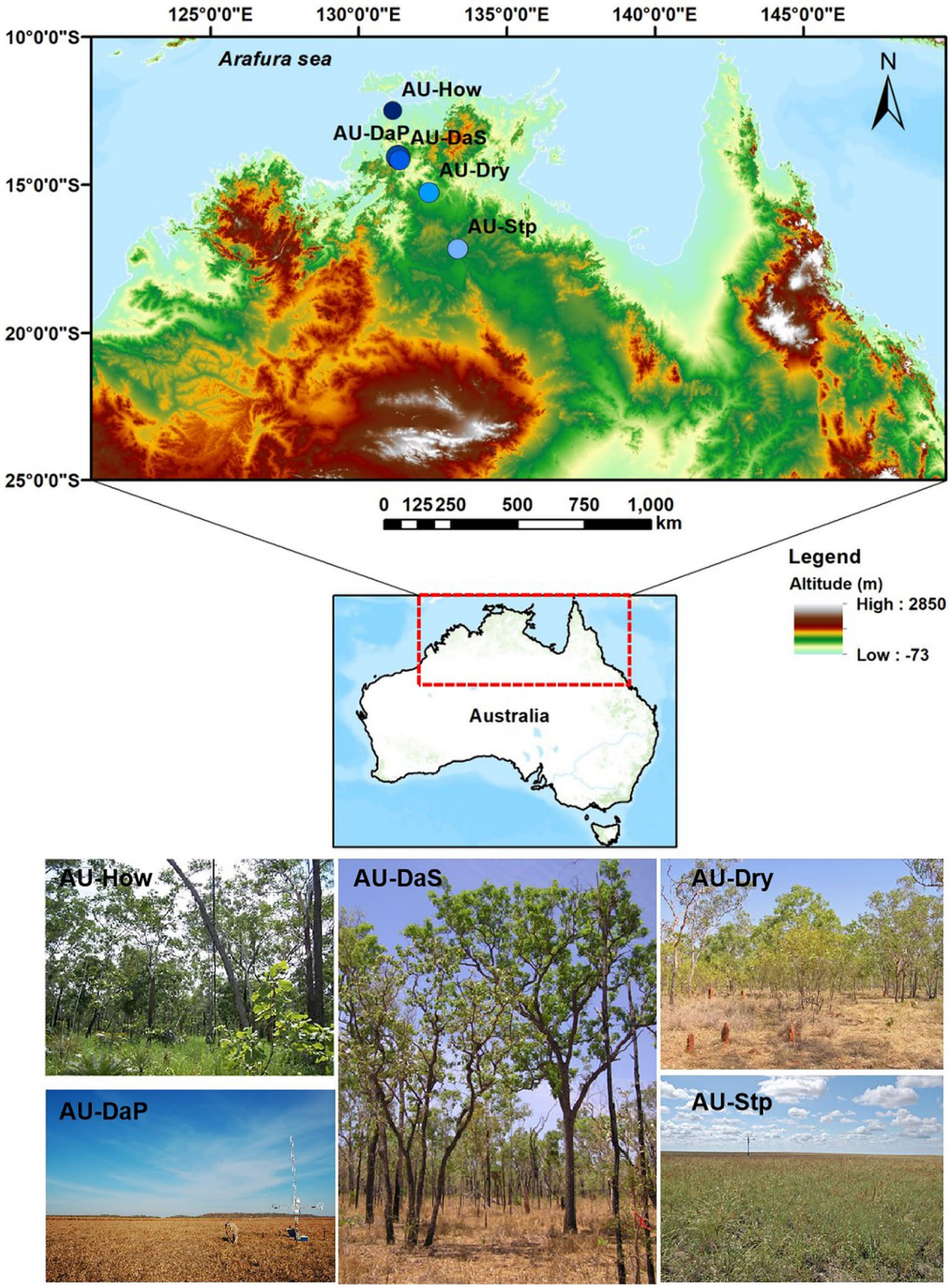

Figure 1. Locations of the five FLUXNET sites used in this study along the North Australian Tropical Transect. Photos are shown to illustrate the differences in the structure of vegetation (http://www.ozflux.org.au/).

Utah, USA), are measured at the depth of 5 cm and/or 15 cm adjacent to the towers. To be consistent, SWC and G data at the depth of 5 and 15 cm, respectively, were used in this study.

To quantify vegetation conditions at the sites, leaf area index (LAI) data were retrieved from the Moderate Resolution Imaging Spectroradiometer (MODIS) MCD15A3H data set (starting in 2002; version 6; https://e4ftl01.cr.usgs.gov/MOTA/), based on the geographical coordinates of each site. The MCD15A3H data set has a temporal resolution of 4 days and a spatial resolution of 500 m, and therefore post-processing was needed to obtain a daily LAI data set. First, based on the quality control information, data with unfavorable conditions (e.g., the presence of cloud and/or snow cover) were filtered out. A cubic smoothing spline method was then used for interpolating the 4-day interval data into daily values (Horn & Schulz, 2010), and the Savitzky-Golay filter was used to smooth out noises in the LAI time series (Chen et al., 2004). At half-hourly timescales, the LAI data remained constant for the analysis during each calendar day.

2.3. Processing of EC Data

The FLUXNET data set has been through rigorous data processing procedures with four main blocks: data quality assurance and control, the Energy & Water Fluxes processing block, the Carbon Fluxes processing block, and the Meteorological Variables processing block (Pastorello et al., 2020; Vuichard & Papale, 2015). The detailed information can be found at https://fluxnet.org/data/fluxnet2015-dataset/data-processing/. Note that the original daytime and nighttime data values in the data set were separated based on the potential incoming shortwave radiation (the theoretical maximum radiation at the top of atmosphere), which was computed using latitude/longitude coordinates and time (Pastorello et al., 2020).

In this study, to ensure the suitability of the EC data for assessing ET_D and ET_N, additional data processing procedures were performed. First, to resolve the energy balance closure problem of EC measurements, the energy closure ratio (ECR) (defined as $(LE + H)/(Rn\text{-}G)$) was computed at annual timescales for each site (Liu et al., 2019). The resulting average annually ECR over the study periods was 0.93, 0.89, 0.91, 0.84, and 0.98 for the AU-How, AU-DaP, AU-DaS, AU-Dry, and AU-Stp site, respectively, which were in accordance with those (0.87 ± 0.15) reported for the FLUXNET sites (Stoy et al., 2013); therefore, no correction was made for closing the energy balance in this study. Second, data records (AU-How: 2001–2014; AU-DaP: 2007–2013; AU-DaS: 2008–2014; AU-Dry: 2008–2014; AU-Stp: 2008–2014) in the first calendar year for each site were omitted (e.g., the year 2001 was removed for the AU-How site) due to the large amount of missing data. Third, LE data were removed if they were collected during stable atmospheric conditions at night according to u^* values. Site-dependent u^* thresholds were determined annually following Reichstein et al. (2005). After the u^* quality filtering, 25.1%, 35.6%, 26.9%, 27.1%, and 39.3% of the original nighttime data were retained for the AU-How, AU-DaP, AU-DaS, AU-Dry, and AU-Stp site, respectively. The percentage of the remaining data for each calendar year at the five FLUXNET sites is provided in Table S2.

To fill the missing nighttime LE data, the online tool (available at https://www.bgc-jena.mpg.de/bgi/index.php/Services/REddyProcWeb) was used. This online gap-filling tool was derived from the technique proposed by Falge et al. (2001), with the consideration of the temporal auto-correction of the fluxes and the co-variations of the fluxes with other meteorological variables (Reichstein et al., 2005). The performance of the gap-filling method was evaluated by comparing observed LE with filled LE according to Moffat et al. (2007), and the results are provided in Table S3. The half-hourly daytime LE (note no gap filling was performed for daytime LE) and gap-filled nighttime LE were used to calculate half-hourly ET_D and ET_N (here, negative values were replaced by zero). Half-hourly data (e.g., ET_D, ET_N and environmental variables at corresponding daytime or nighttime) were then summed up to obtain daily, monthly, and annual values. As dew formation might be important in some areas (Groh et al., 2019; Jacobs et al., 2006), the half-hourly gap-filled LE with negative values were also summed up to compute the amount of dew formation at the sites.

2.4. Statistical Analysis

The BRT method developed by Elith et al. (2008) was applied to quantify how environmental factors influenced half-hourly ET_D and non-gap-filled ET_N (calculated from nongap-filled half-hourly nighttime LE) along the climate gradient of the NATT. As a nonlinear machine learning method, the BRT method differs

from traditional regression methods in that it uses the boosting technique to adaptively combine large numbers of relatively simple tree models for predicting the relationship between predictor and response variables (Elith et al., 2008). Specifically, based on the recursive binary splitting method, tree-based models are fitted iteratively to the observations, until a minimum deviance is reached between observed and predicted data. The relative impact of a predictor variable on a response variable is quantified based on the number of times the predictor variable is used for splitting the trees, which is then weighted by the squared improvement to the whole tree-based model (Breiman et al., 1984). The BRT method does not require any specific data distributions, and thus is suitable for analyzing datasets with outliers, interactions among predictor variables, and missing data (Elith et al., 2008).

The open-source BRT package developed by Elith et al. (2008) was employed in this study using the R software (version 3.5.1, R Core Team, 2018), which requires four key input parameters (i.e., learning rate-*lr*, tree complexity-*tc*, number of trees-*nt*, and bag fraction-*bg*). The parameters *lr* and *tc* determine the contribution of individual trees to the growing model and the structure of a tree, respectively, which jointly determine *nt* for optimal predictions. The maximum and minimum *nt* values were set to be 30,000 and 1,000, respectively, as suggested by Elith et al. (2008). Moreover, the stochasticity of the boosted model is controlled through *bg* that specifies the proportion of data to be selected at each iteration from the full training set. To obtain optimal predictive results, combinations of parameter values (e.g., *lr* [0.003, 0.005, 0.01, 0.03, 0.05], *tc* [from 7 to 10 by an increment of 1], and *bg* [0.5, 0.75]) were tested (Liu et al., 2019), and an optimal parameter set, which provided the minimum predictive deviance between observed and predicted data, was chosen for each site to compute the relative contribution of each predictor variable in controlling ET_D and ET_N.

Following Elith et al. (2008), a 10-fold cross-validation method was used to build the BRT model and assess its performance. Data were first randomly partitioned into 10 subsets, with 9 subsets for training the model and the remaining one for testing the model performance. This procedure was repeated 10 times to get the predictive results. Note that the multicollinearity in predictor variables (e.g., *Rn*, SWC, LAI, VPD, T_a, and WS) may affect the performance of the BRT model for predicting response variables (e.g., ET_D and ET_N). To resolve this issue, Pearson's correlation coefficient (r) and variance inflation factor (VIF) analysis (i.e., $|r| < 0.7$ and $VIF < 5$) were used to test the multicollinearity among predictor variables (Dormann et al., 2013). The performance of the BRT model was evaluated using the Nash-Sutcliffe efficiency, root mean square error, and coefficient of determination by comparing observed and modeled half-hourly ET_D and ET_N for each site (Table S4).

3. Results and Discussion

3.1. Mean Annual ET_D and ET_N Patterns Along the Climate Gradient

3.1.1. Spatial Variability in Mean Annual ET_D and ET_N

Along the NATT from AU-How to AU-Stp, $\overline{P}$ decreased from 1715.5 mm/year to 761.1 mm/year during the study periods, while mean annual potential evapotranspiration ($\overline{ET_p}$) (calculated by the Penman-Monteith equation [Allen et al., 1998]) showed an opposite trend from 1689.5 mm/year to 2146.2 mm/year; accordingly, mean annual aridity index ($\overline{ET_p}/\overline{P}$) varied from 0.98 to 2.82. The mean annual dew formation was about 4.5 mm/year at the sites, which was negligible compared to the values reported for humid grassland sites in Germany (Groh et al., 2019) and forested sites in central Colorado (Berkelhammer et al., 2013). Thus, the impact of dew formation was not considered in this study; however, it should be noted that the amount of dew formation was inferred based on the EC measurements, which might lead to uncertainties in the dew formation estimates (Moro et al., 2007). Nevertheless, the pronounced climate gradient along the NATT is ideal for diagnosing the responses of ET_D and ET_N to varying climatic conditions.

Among the five sites, $\overline{ET}$ varied from 1158.2 mm/year at AU-How in the north to 609.7 mm/year at AU-Stp in the south, which expectedly was primarily composed of ET_D (Table 2). Intriguingly, it appeared that $\overline{ET_D}$ exhibited a stronger variation than $\overline{ET_N}$ along the NATT. For demonstration, Figures 2a–2l show the relationships of $\overline{ET_D}$ and $\overline{ET_N}$ with different environmental variables across the sites. In general, the correlations of $\overline{ET_D}$ with meteorological and vegetation variables were notable, while $\overline{ET_N}$ only showed good relationships with $\overline{T_a}$ and $\overline{Rn}$, illustrating the contrasting responses of $\overline{ET_D}$ and $\overline{ET_N}$ to the environmental

Table 2
Mean Annual Actual Evapotranspiration ($\overline{ET}$), Daytime Evapotranspiration ($\overline{ET_D}$), Nighttime Evapotranspiration ($\overline{ET_N}$), and ET_N/ET_D ($\overline{ET_N}$ / $\overline{ET_D}$) for the Five Study Sites Along the North Australian Tropical Transect

Site ID	$\overline{ET}$(mm/year)	$\overline{ET_D}$(mm/year)	$\overline{ET_N}$(mm/year)	$\overline{ET_N}$ / $\overline{ET_D}$(%)
AU-How	1158.2 (1004.5–1413.4)[a]	1090.9 (928.2–1319.8)	67.2 (45.8–93.6)	6.2 (4.6–8.2)
AU-DaP	749.3 (611.4–915.8)	712.1 (592.9–861.6)	37.3 (18.6–54.2)	5.1 (2.8–6.6)
AU-DaS	930.9 (882.8–972.6)	849.0 (819.1–882.7)	81.9 (63.6–91.3)	9.6 (7.8–10.8)
AU-Dry	884.4 (804.3–1164.4)	802.5 (728.7–1069.3)	81.9 (74.0–95.2)	10.3 (8.9–12.3)
AU-Stp	609.7 (467.3–854.3)	546.4 (413.7–771.9)	63.2 (40.3–82.5)	11.7 (7.9–14.2)

[a]The range of annual variables during the study period.

gradient. In particular, the correlation between $\overline{ET_N}$ and $\overline{P}$ was significantly lower than that between $\overline{ET_D}$ and $\overline{P}$ (Figures 2b and 2h). This suggests that as atmospheric demands for ET became lower at night, the constraint of water supplies (indicated by $\overline{P}$ levels) on ET_N weakened. Instead, $\overline{ET_N}$ across the sites was dominantly controlled by $\overline{T_a}$ (most likely through affecting soil evaporation; Liu et al., 2015). As such, the narrow $\overline{T_a}$ range led to a relatively weaker variation in $\overline{ET_N}$ along the NATT.

With higher atmospheric demands for ET_D (especially due to enhanced daytime plant *Tr*; see Table 1 for daytime $\overline{Tr}/\overline{ET}$), the impacts of vegetation (e.g., $\overline{LAI}$) and relevant meteorological variables (e.g., $\overline{VPD}$) on $\overline{ET_D}$ emerged across the sites. These factors with large variabilities led to a stronger variation in $\overline{ET_D}$ along the NATT. Nevertheless, the data along the NATT provided strong observational evidence that $\overline{ET_D}$ and $\overline{ET_N}$ could respond differently to the climate gradient with $\overline{ET_D}$ showing more distinct interactions with influencing factors, primarily due to the increased daytime plant *Tr*.

3.1.2. Environmental Controls on Mean Annual ET_N/ET_D Ratios

The ratio of ET_N/ET_D (or ET_N/ET) is an important metric for quantifying the relative importance of nighttime water loss over terrestrial ecosystems (Dawson et al., 2007; Groh et al., 2019; Iritz & Lindroth, 1994; Novick et al., 2009; Padrón et al., 2020). With the pronounced climate and vegetation gradients along the NATT, the $\overline{ET_N}/\overline{ET_D}$ ratio varied noticeably among the sites (Table 2), which were comparable to previous studies. For instance, Tr_N was 5%–15% of daytime Tr in a eucalypt woodland in Western Australia (Dawson et al., 2007); grass and tree ecosystems in the Southeastern USA exhibited annual ET_N/ET_D of 8%–9% using EC measurements (Novick et al., 2009). The relationships of $\overline{ET_N}/\overline{ET_D}$ with different environmental variables are presented in Figures 2m–2r. Interestingly, although $\overline{T_a}$ and $\overline{Rn}$ were the leading controls on $\overline{ET_N}$ as shown above, their relationships with $\overline{ET_N}/\overline{ET_D}$ deteriorated significantly. Instead, the strong correlations of $\overline{ET_N}/\overline{ET_D}$ with $\overline{P}$, $\overline{VPD}$, and $\overline{LAI}$ mainly reflected the spatial variation in $\overline{ET_D}$ along the NATT. By contrast, Zeppel et al. (2010) reported that Tr_N mostly determined the seasonal variation in ET_N/ET_D in a eucalypt-dominated woodland in New South Wales, Australia. Thus, it is reasonable to postulate that the contrasts in $\overline{ET_D}$ and $\overline{ET_N}$ responses to climatic drivers, which can be further complicated by vegetation conditions, can greatly mask the relationships of $\overline{ET_N}/\overline{ET_D}$ (or $\overline{ET_N}/\overline{ET}$) with $\overline{P}$ and $\overline{T_a}$ among different climate regimes and ecosystems, making it difficult to seek a general pattern of $\overline{ET_N}/\overline{ET}$ with environmental variables at the global scale as demonstrated by Padrón et al. (2020).

3.2. Monthly and Annual Variations in ET_D and ET_N

Monthly ET_D and ET_N showed clear seasonal patterns with higher values occurring in wet seasons (Figures 3a and 3b). Note that Groh et al. (2019) reported higher ET_N during nongrowing seasons, mostly due to longer nocturnal hours in winter times at the authors' study sites. In contrast, the nocturnal hours at the sites in Northern Australia are similar among different seasons. Moreover, with the pronounced climate seasonality, the temporal variations in monthly ET_D and ET_N at site levels showed good correlations with

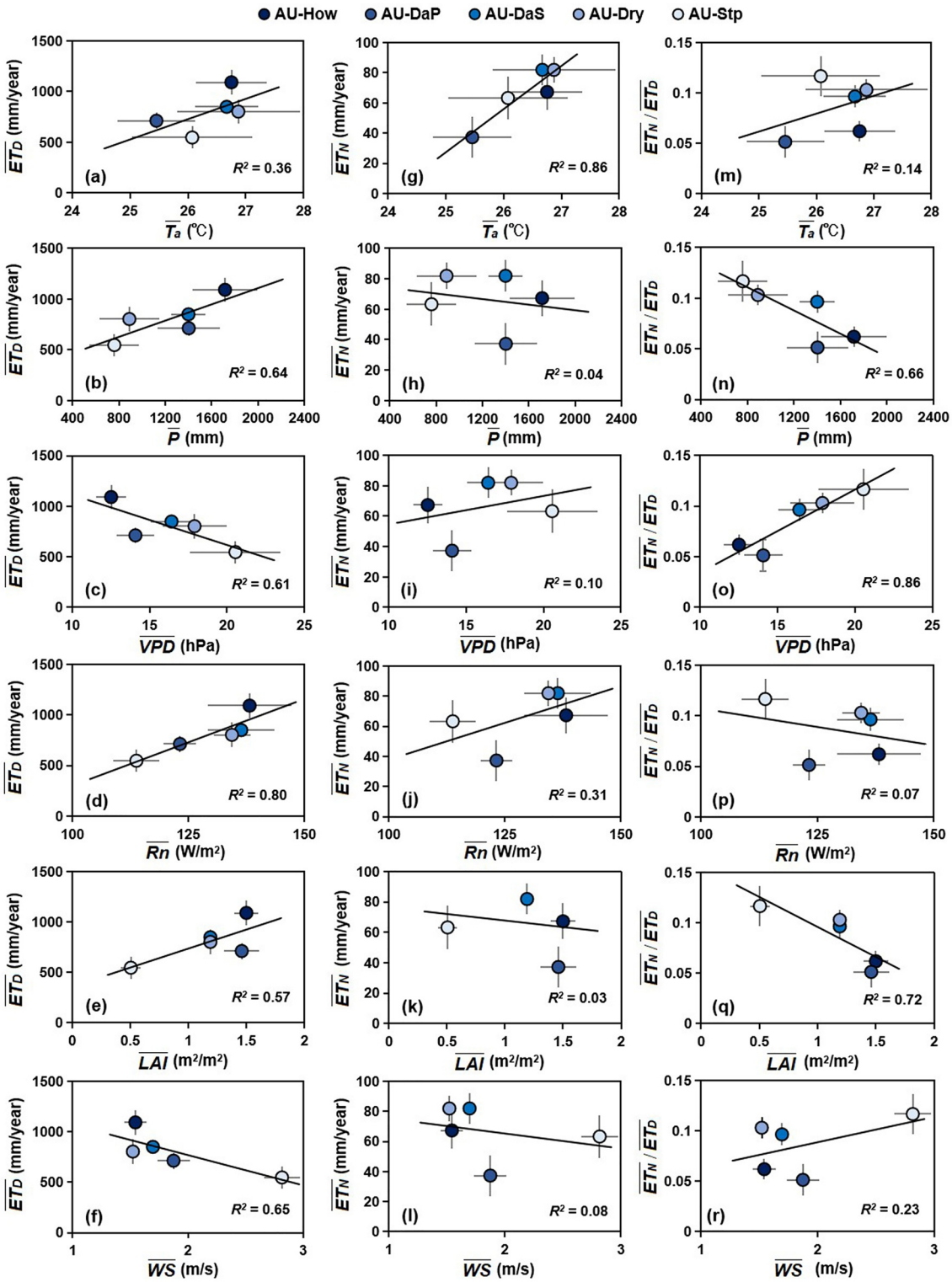

Figure 2. Relationships of mean annual air temperature ($\overline{T_a}$), precipitation ($\overline{P}$), vapor pressure deficit ($\overline{VPD}$), net radiation ($\overline{Rn}$), leaf area index ($\overline{LAI}$), and wind speed ($\overline{WS}$) with mean annual daytime and nighttime evapotranspiration ($\overline{ET_D}$, $\overline{ET_N}$) for the five study sites encoded by gradient colors (annual mean ± standard deviation).

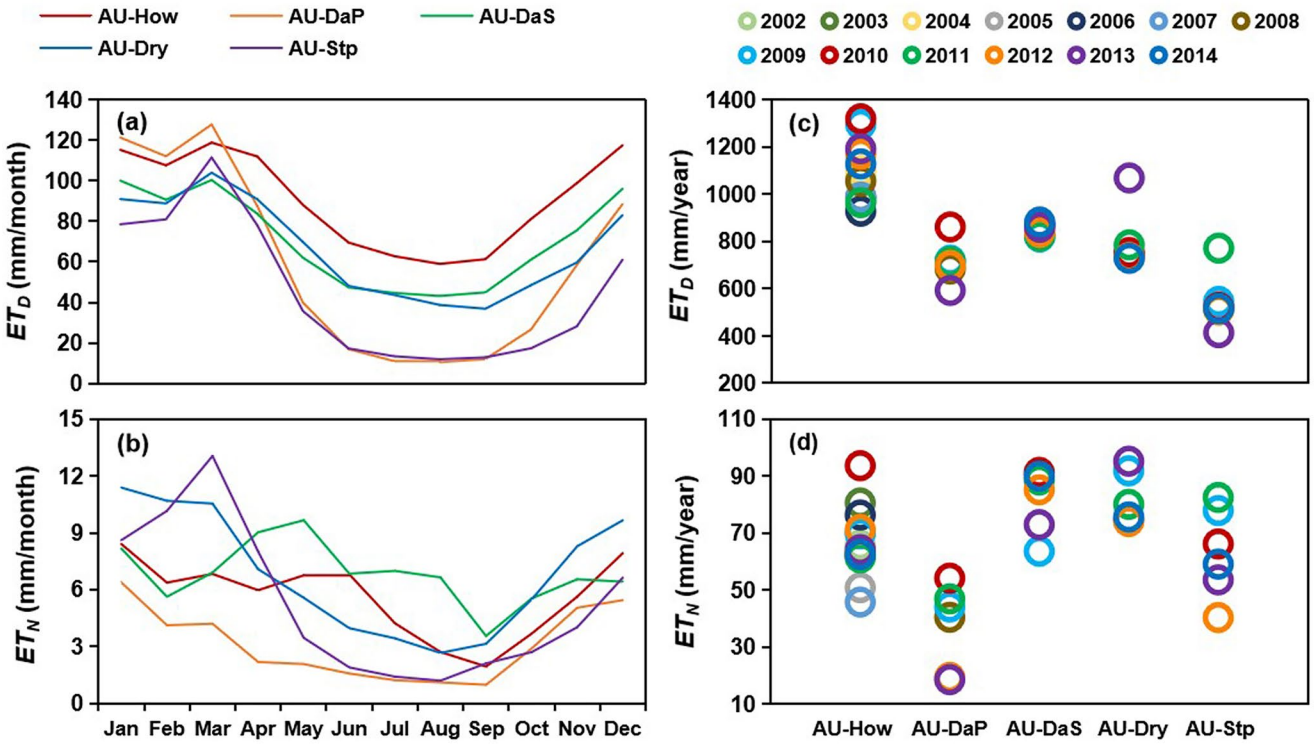

Figure 3. Average monthly daytime and nighttime evapotranspiration (ET_D, ET_N) and interannual variations in ET_D and ET_N for the five study sites.

meteorological and vegetation variables (Table 3; except for ET_N at AU-DaS). In particular, LAI and SWC were the leading factors of ET_D, and ET_N dynamics were dominated by SWC. Note that although $\overline{T_a}$ largely determined the spatial variability in $\overline{ET_N}$ along the NATT, local T_a became relatively less important in controlling monthly ET_N variations at each individual site.

Monthly ET_D and ET_N at each site were positively correlated with each other (Figure 4), which was in line with previous findings (Cavenderbares et al., 2007; Novick et al., 2009). Interestingly, the correlation between monthly ET_D and ET_N became progressively stronger with increasing climate dryness across the sites (as indicated by aridity index; except for AU-DaS). It suggested a stronger coupling between monthly ET_D and ET_N under drier climatic conditions, as monthly ET_D and ET_N showed more similar responses to environmental drivers at drier sites (Table 3). Recent investigation revealed that higher daytime photosynthetic rates generally led to higher Tr_N, due to the endogenous circadian rhythm of plant physiological activities (O'keefe & Nippert, 2018; Resco De Dios et al., 2015). To some degree, the strong correlations between monthly ET_D and ET_N in our results (Figures 3a, 3b and 4) supported this claim, which might be also affected by climatic conditions.

Interannual variability in ET is a longstanding research question as it is related to the critical roles of climate interannual variability in controlling annual variations in hydrological processes and biomass production (Fatichi & Ivanov, 2014; Milly & Dunne, 2002). As shown in Table 3, no strong correlations could be found to indicate the dominant factors driving the interannual variations in ET_D and ET_N at the study sites, although it is interesting to note that annual ET_N appeared to show relatively larger year-to-year variations than ET_D (Figures 3c and 3d). In general, LAI and SWC played important roles in determining ET_D variations, while the influencing factors of ET_N depended on ecosystem types, SWC for grass sites and meteorological variables (i.e., Rn, VPD, and T_a) for savanna sites. Compared to the monthly data, the results suggested the decoupling of ET_D and ET_N with environmental variables at longer timescales (Table 3); however, it might also be attributed to the fact that the length of data records might not be long enough to reveal annual patterns of ET_D and ET_N with those variables. It is likely that different responses of ET_D and ET_N to environmental

Table 3
Spearman Correlation of Daytime and Nighttime Evapotranspiration (ET_D, ET_N) With Air Temperature (T_a), Vapor Pressure Deficit (VPD), Soil Water Content (SWC), Net Radiation (Rn), Leaf Area Index (LAI), and Wind Speed (WS) for the Five Study Sites at Different Timescales Along the North Australian Tropical Transect

		Daily		Monthly		Annual	
Site ID	Variables	ET_D	ET_N	ET_D	ET_N	ET_D	ET_N
AU-How	T_a	0.37[a]	0.13[a]	0.29[a]	0.18[b]	0.15	0.25
	VPD	−0.29[a]	−0.14[a]	−0.65[a]	−0.36[a]	−0.18	0.22
	SWC	0.53[a]	0.43[a]	0.71[a]	0.51[a]	−0.05	−0.25
	Rn	0.45[a]	0.23[a]	0.20[b]	0.35[a]	0.27	0.67[b]
	LAI	0.55[a]	0.23[a]	0.62[a]	0.34[a]	0.48	0.16
	WS	−0.14[a]	0.19a	−0.38[a]	0.17[b]	−0.005	0.23
AU-DaP	T_a	0.14[a]	0.33[a]	0.13	0.38[a]	−0.14	−0.20
	VPD	−0.56[a]	−0.35[a]	−0.72[a]	−0.51[a]	−0.26	−0.54
	SWC	0.75[a]	0.62a	0.81[a]	0.69[a]	0.26	0.66
	Rn	0.42[a]	0.38[a]	0.26[b]	0.48[a]	0.20	−0.37
	LAI	0.80[a]	0.41[a]	0.84[a]	0.47[a]	0.31	0.31
	WS	−0.27[a]	0.06[a]	−0.44[a]	0.003	0.6	−0.09
AU-DaS	T_a	0.40[a]	−0.20[a]	0.39[a]	−0.24[b]	0.14	0.49
	VPD	−0.26[a]	−0.04	−0.57[a]	−0.21	−0.03	−0.14
	SWC	0.63[a]	0.21[a]	0.77[a]	0.25[b]	−0.09	0.37
	Rn	0.63[a]	−0.07[a]	0.66[a]	0.03	0.54	0.26
	LAI	0.64[a]	−0.13[a]	0.80[a]	−0.12	0.81[b]	0.35
	WS	−0.30[a]	0.11[a]	−0.61[a]	−0.03	−0.20	−0.60
AU-Dry	T_a	0.09[a]	0.27[a]	0.07	0.34[a]	0.09	0.20
	VPD	−0.34[a]	−0.41[a]	−0.53[a]	−0.55[a]	−0.43	0.54
	SWC	0.74[a]	0.73[a]	0.79[a]	0.81[a]	0.60	0.43
	Rn	0.40[a]	0.51[a]	0.46[a]	0.74[a]	0.09	0.26
	LAI	0.58[a]	0.34[a]	0.68[a]	0.47[a]	−0.09	0.06
	WS	−0.37[a]	−0.14[a]	−0.72[a]	−0.39[b]	−0.71	0.60
AU-Stp	T_a	0.16[a]	0.27[a]	0.22	0.45[a]	−0.49	−0.26
	VPD	−0.29[a]	−0.44[a]	−0.40[a]	−0.43[a]	−0.66	−0.26
	SWC	0.71[a]	0.63[a]	0.79[a]	0.76[a]	0.89[b]	0.77
	Rn	0.51[a]	0.50[a]	0.71[a]	0.79[a]	−0.09	0.26
	LAI	0.65[a]	0.42[a]	0.70[a]	0.49[a]	0.70	0.55
	WS	−0.11[a]	−0.01	−0.38[a]	−0.26[b]	0.49	0.37

[a]Correlation is significant at the 0.01 level (two-tailed). [b]Correlation is significant at the 0.05 level (two-tailed).

drivers at site levels led to the varying degrees of the coupling strength between ET_D and ET_N at different temporal scales (monthly vs. annual timescales).

3.3. ET_D and ET_N Behaviors With Environmental Drivers at Daily Timescales

The relationships of daily ET_D and ET_N with environmental variables show similar patterns for the five sites (Table 3). During daytime, both LAI and SWC were the leading controls on daily ET_D with SWC being more important at drier sites (i.e., the AU-Dry and AU-Stp sites). Similar conclusions have been reached in previous studies (Han et al., 2020; Williams & Torn, 2015). By comparison, the correlations of LAI with daily ET_N considerably weakened, while the correlations between SWC and daily ET_N also weakened, but to lesser

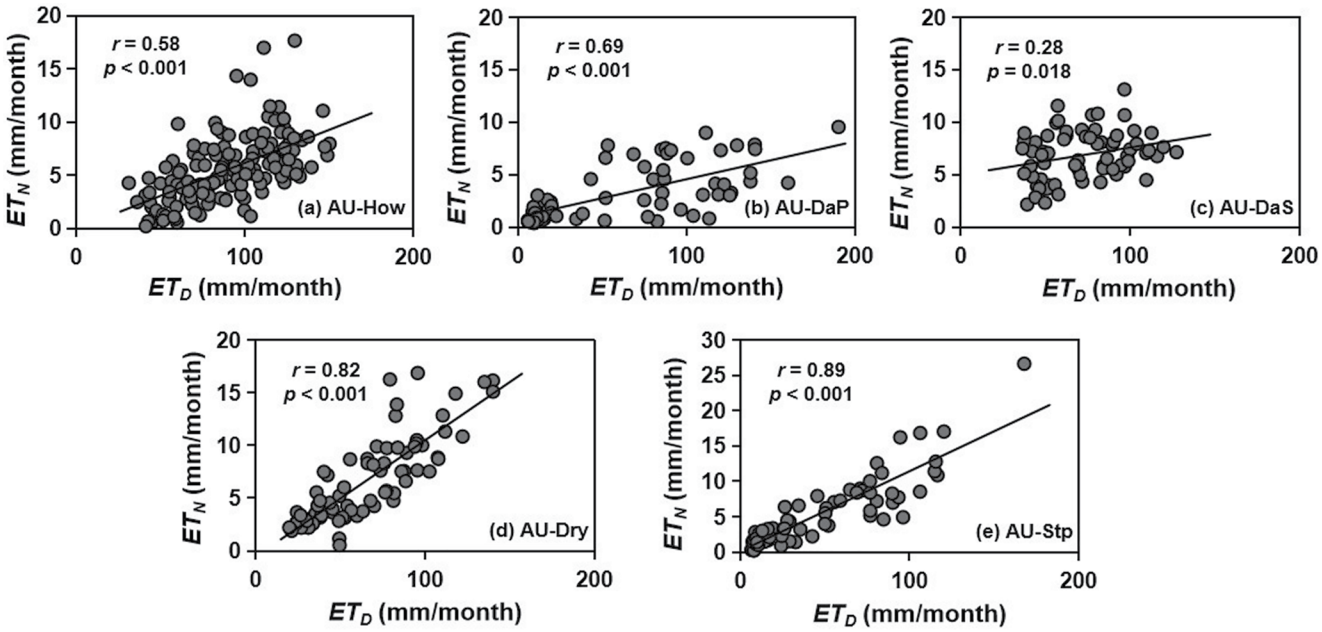

Figure 4. Relationships between monthly daytime evapotranspiration (ET_D) and nighttime evapotranspiration (ET_N) for the five study sites. r is the Pearson's correlation coefficient.

degrees. However, as SWC and VPD at daily timescales were strongly coupled (Figure S1), it is possible that the strong correlations of SWC with daily ET_D and ET_N were the byproduct of the impact of VPD on daily ET. Therefore, the responses of daily ET_D and ET_N to SWC and VPD require further investigation.

The question as to the relative importance of SWC and VPD in determining terrestrial land surface processes, such as ET and biomass production, is an ongoing debate in climate change studies (Liu et al., 2020; Novick et al., 2016; Sulman et al., 2016). To address this issue, Figure 5 shows the relationship of ET_D or ET_N with daytime or nighttime SWC (SWC_D and SWC_N, respectively) at the study sites. Overall, below certain SWC thresholds, ET_D* was enhanced with increasing SWC_D, due to the constraint of water supplies on ET; whereas, SWC_D started to show a damping effect on ET_D* when the thresholds were crossed, implying that factors other than SWC_D primarily affected ET_D (e.g., VPD; see the following analysis). With less atmospheric demands for ET_N, the threshold behavior of ET_N* with SWC_N became less pronounced, suggesting that daily ET_N was less responsive to the change in SWC levels.

The threshold, at which daily ET starts to decrease with increasing SWC, is determined by a suite of variables, such as soil properties, meteorological conditions, and vegetation characteristics (Haghighi et al., 2018; Vivoni et al., 2008). For instance, there was no clear threshold at AU-Stp (Figure 5e). With the driest climate and highest atmospheric water demands, SWC was the primary factor controlling ET. By comparison, the threshold was smallest at AU-DaS among the five sites (Figure 5c), likely due to the coarse soil texture with a low water holding capacity as indicated by the lowest average level of SWC at this site (e.g., the sand fraction was 63% by weight according to the soil database of Shangguan et al., 2014). It is worth noting that with ~13.4 km apart, the AU-DaS and AU-DaP sites received similar $\overline{P}$; however, both $\overline{ET_D}$ and $\overline{ET_N}$ were substantially higher at AU-DaS with lower SWC levels (Table 2), where deep-rooted trees could access deeper soil moisture for ET (as indicated by the canopy height in Table 1).

The above results underscored the necessity of combining the effects of SWC and other influencing factors for elucidating daily ET_D and ET_N dynamics (e.g., explaining the damping effect of SWC on ET). For simplicity, all observed data from the five sites were synthesized together to show the combined impact of SWC and VPD on daily ET_D and ET_N in Figure 6. At low daytime VPD (VPD_D; e.g., below ~15 hPa), daily ET_D tended to increase rapidly with increasing VPD_D, as VPD can act as a driving force for stomatal water fluxes (Gu et al., 2006); whereas, their relationship became negative when VPD_D exceeded a critical value, due to stomatal regulation and the limitation of SWC (Gu et al., 2006; Leuning, 1995; Song et al., 2020). Note

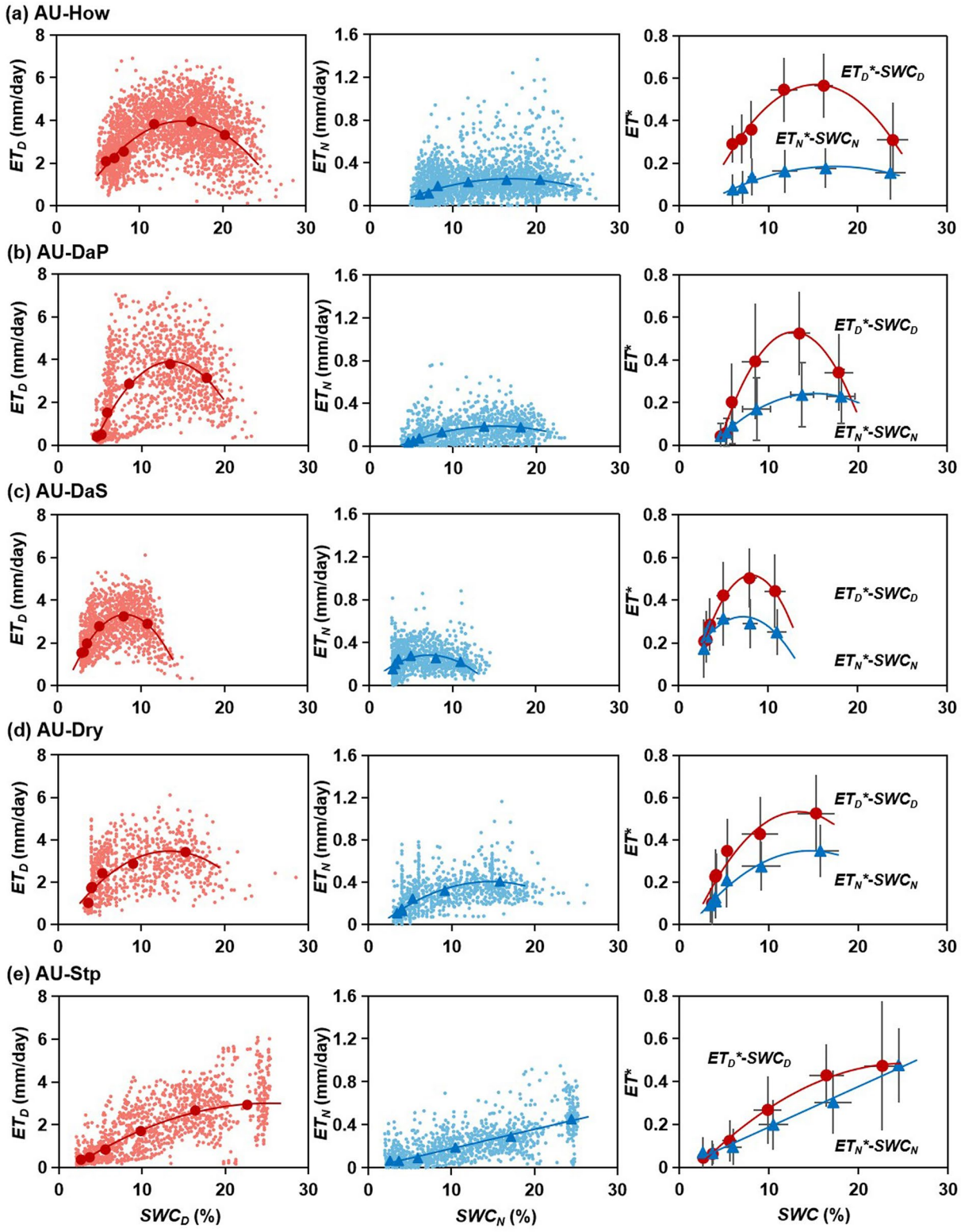

Figure 5. Relationships of daytime and nighttime soil water content (SWC_D, SWC_N) with daytime and nighttime evapotranspiration (ET_D, ET_N) at daily timescales. The data were binned according to the *SWC* range. Normalized daily ET_D and ET_N (ET_D*, ET_N*; that is, $(ET - ET_{min})/(ET_{max} - ET_{min})$, where ET_{max} and ET_{min} are the maximum and minimum observed ET_D or ET_N during the study periods, respectively) are also given here. Polynomial curves are fitted through the average points, and horizontal and vertical bars represent standard deviations of *SWC* and *ET**, respectively.

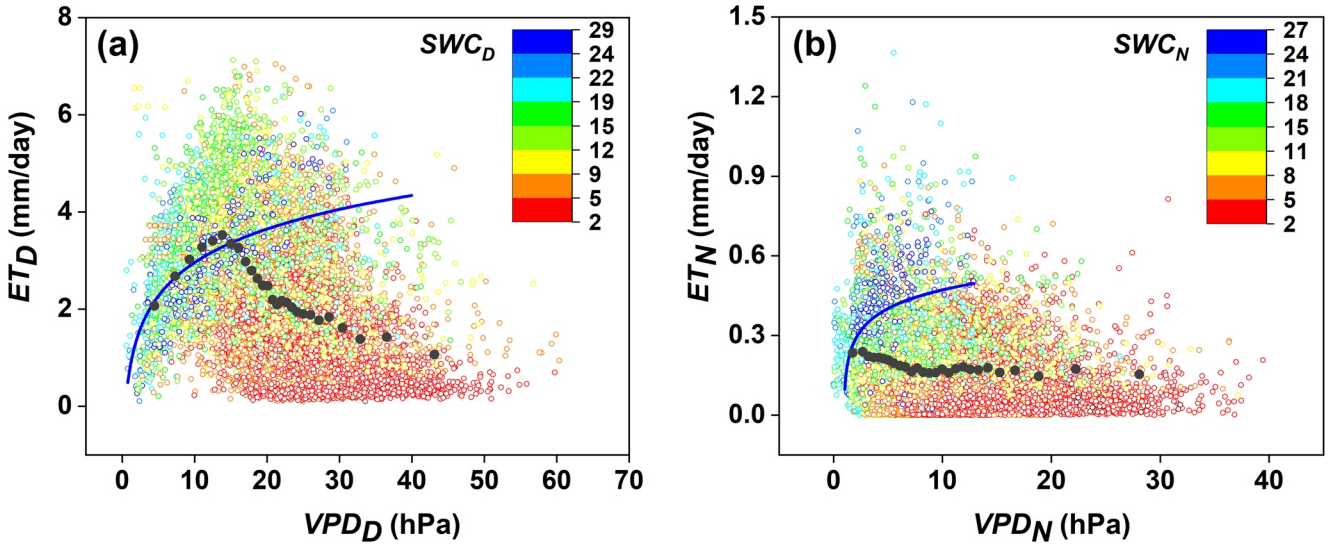

Figure 6. Relationships between daily vapor pressure deficit (VPD) and evapotranspiration (ET) under different soil water content (SWC) levels in the daytime (*D*; a) and at night (*N*; b) for the five study sites. The blue line was fitted with data of SWC > 24% (here, SWC = 24% was used for a demonstration purpose). The gray scatters were obtained by averaging every 500 points after sorting by VPD in a positive sequence.

that the hysteresis between ET and VPD has been suggested, which is regulated by biotic factors (e.g., leaf water potential) and abiotic factors (e.g., soil water status) (Zhang et al., 2014); however, this is beyond the scope of this study. In contrast, daily ET_N showed less response to nighttime VPD or even a negative pattern, which agreed well with previous studies (Barbour & Buckley, 2007; Resco De Dios et al., 2015). Since soil evaporation becomes more important in contributing to ET at night due to reduced plant *Tr*, the control of VPD on ET_N weakens (as shown here) in that VPD mainly affects ET through regulating stomatal water fluxes (Gu et al., 2006). The lower sensitivity of ET_N to VPD in our study was partly inconsistent with some previous findings, which might be due to different physiological strategies among different plant species (e.g., isohydric and anisohydric behaviors) (Ogle et al., 2012; O'keefe & Nippert, 2018). Moreover, when SWC was no longer a limiting factor for ET (SWC > 24%), both ET_D and ET_N were positively correlated with VPD, attesting the interacting effect of VPD and SWC on ET processes.

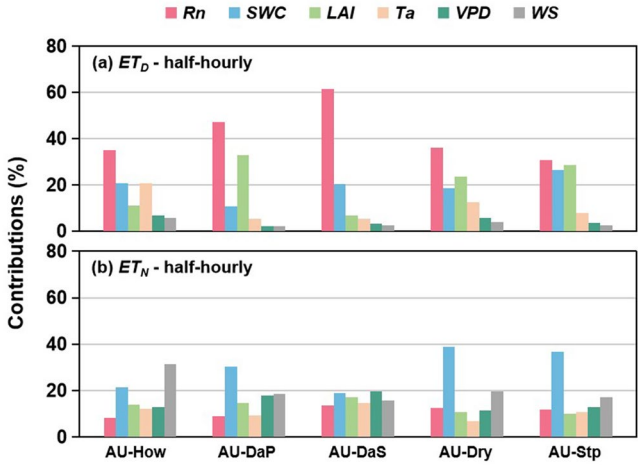

Figure 7. Relative contributions of net radiation (Rn), soil water content (SWC), leaf area index (LAI), air temperature (T_a), vapor pressure deficit (VPD), and wind speed (WS) to half-hourly daytime and non-gap-filled half-hourly nighttime evapotranspiration (ET_D, ET_N) for the five study sites from the boosted regression tree (BRT) analysis.

3.4. Quantification of Environmental Variables for Controlling Half-Hourly ET_D and ET_N Dynamics

Figure 7 compares the relative contributions of different environmental factors to half-hourly ET_D and nongap-filled half-hourly ET_N variations at each site based on the BRT results. The BRT results showed good agreement between observed and modeled half-hourly ET_D and ET_N (Table S4), illustrating the viability of using the BRT method for predicting ET_D and ET_N in the study region. During daytime, Rn was the dominant control at half-hourly timescales at the study sites, which supported recent findings that energy played more important role than water in regulating ET at diurnal timescales around the globe (for example, Huang et al., 2019; Scott & Biederman, 2019). Note that the high contribution of Rn at AU-DaS was also consistent with the results shown in Figure 5, as the access to deeper soil moisture by deep-rooted trees at this site would alleviate the constraint of water supplies for ET throughout the year, resulting in the increased contribution of *Rn*. In addition, LAI was also an important

contributor at the grassland sites (i.e., AU-DaP and AU-Stp), which was consistent with the reports of Williams and Torn (2015) and Han et al. (2020).

By comparison, the contrasts in the relative contributions of different variables to ET_N were less than to ET_D, suggesting that ET_N had more complex interactions with the surrounding environment. Particularly, half-hourly ET_N dynamics were mainly controlled by SWC and WS across the sites. For WS, the aerodynamic resistance that is related to WS regulates the water vapor transfer rate as a physical mechanism, and the wind can also prevent the formation of an intense nighttime inversion above the canopy (Green et al., 1989; Malek, 1992). In particular, at AU-How that is located offshore, the humid climate tended to promote the tight coupling between wind and ET_N (Meinzer et al., 1995).

3.5. Ecohydrological Implications

Increasing observational and numerical modeling evidence has indicated the important role played by ET_N in modulating terrestrial land surface and ecohydrological processes. The results of this study showed that long-term $\overline{ET_N}/\overline{ET_D}$ was averaged at 8.6% along the NATT climate gradient. As a nonnegligible component of terrestrial ET, this has important implications for water resources management, particularly in arid regions as $\overline{ET_N}/\overline{ET_D}$ increased with climate dryness. For instance, $\overline{ET_N}$ (81.9 mm/year) at AU-Dry was about 3.6 times higher than the long-term surface runoff (~23 mm/year) observed by Jolly (2002) in the Dry River area, where the AU-Dry site is located.

Additionally, the observational data showed that the responses of ET_D and ET_N were different to environmental drivers at the study sites. For instance, at mean annual timescales, both vegetation and climatic conditions (e.g., $\overline{P}$ and $\overline{VPD}$) were closely related to $\overline{ET_D}$ variations across the sites, while $\overline{ET_N}$ only varied with $\overline{T_a}$. As ET is one of the main subjects in climate change studies (Fisher et al., 2017; Novick et al., 2016), the differences in the nonlinear responses of ET_D and ET_N to those environmental drivers would have different consequences for regional and global water balances. Therefore, to improve our understanding of future climate change and its impact on hydrological cycles, ET_D and ET_N should be investigated separately.

Finally, we demonstrated that dominant controls on ET_D and ET_N also varied with temporal scales. For instance, ET_N dynamics were dominated by SWC from half-hourly to monthly timescales, while the primary controls on ET_N switched to SWC or energy supplies at annual timescales and to $\overline{T_a}$ at mean annual timescales. As the selection of input variables needs to consider multitemporal scale correlations of ET with environmental drivers for land surface and climate models (Baldocchi & Wilson, 2001; Ogée et al., 2003), our data further showed that those multitemporal scale correlations occurred in both ET_D and ET_N. Furthermore, as ET and gross primary productivity (GPP) are strongly correlated, the different controlling mechanisms of ET (both ET_D and ET_N) across temporal scales would affect the relative importance of multiple environmental factors to GPP variations over a wide range of timescales (Baldocchi & Wilson, 2001; Domec et al., 2012). This is critical for understanding water and carbon cycles in terrestrial ecosystems, particularly in light of changing climatic conditions.

4. Conclusions

Long-term EC records at five FLUXNET sites along a climate gradient in Northern Australia were analyzed to compare the responses of ET_D and ET_N to environmental variables at different temporal scales. The main conclusions of this study are as follows:

1. At mean annual timescales, as $\overline{P}$ largely determined vegetation distributions in the study region, both vegetation and climatic conditions were closely related to $\overline{ET_D}$ variations across the sites. From annual to daily timescales, water supplies (SWC) and vegetation conditions (LAI) controlled ET_D dynamics with SWC being more important at drier sites; whereas, at half-hourly timescales, meteorological conditions (mostly Rn) regulated ET_D
2. Compared to ET_D, ET_N was shown to be less responsive to environmental variables. At mean annual timescales, the primary controls on $\overline{ET_N}$ were $\overline{T_a}$ and $\overline{Rn}$, suggesting that with lower atmospheric water demands at night, the constraint of water supplies on $\overline{ET_N}$ weakened. At annual timescales, the

controlling factors of ET_N depended on ecosystem types, SWC for grass sites and meteorological variables (i.e., *Rn*, VPD, and T_a) for savanna sites. From monthly to half-hourly timescales, ET_N dynamics were dominated by SWC

3. At site levels, monthly ET_D and ET_N showed better correlations with meteorological and vegetation variables than annual ET_D and ET_N, and the coupling of ET_D and ET_N was also stronger at monthly timescales, particularly under drier climatic conditions. In addition, the responses of daily ET_D and ET_N to SWC exhibited similar threshold behaviors with higher sensitivities of daily ET_D to changes in SWC; whereas, daily ET_D and ET_N responded differently to VPD, especially under low VPD levels.

The above results proved our hypothesis that ET_D and ET_N had different responses to environmental drivers across diverse climate regimes and ecosystems at varying temporal scales. Our study provides a critical evaluation for contrasting ET_D and ET_N interactions with constantly changing environments, which has important implications for ecosystem water balance and land surface processes modeling.

Data Availability Statement

Eddy covariance data are available at https://fluxnet.org/data/fluxnet2015-dataset/, and LAI data are available at https://e4ftl01.cr.usgs.gov/MOTA/.

Acknowledgments
This work used eddy covariance data acquired and shared by the FLUXNET community, including OzFlux-TERN networks. The ERA-Interim reanalysis data are provided by ECMWF and processed by LSCE. The FLUXNET eddy covariance data processing and harmonization was carried out by the AmeriFlux Management Project, and Fluxdata project of FLUXNET, with the support of CDIAC and ICOS Ecosystem Thematic Center, and the OzFlux offices. This study was supported by National Key R&D Program of China (2019YFC1804400) and National Natural Scientific Foundation of China (Grant No. U1612441 and 41977161). T. Wang acknowledges the financial support from the Thousand Talent Program for Young Outstanding Scientists and from Tianjin University.

References

Agam, N., Evett, S. R., Tolk, J. A., Kustas, W. P., Colaizzi, P. D., Alfieri, J. G., et al. (2012). Evaporative loss from irrigated interrows in a highly advective semi-arid agricultural area. *Advances in Water Resources*, *50*, 20–30. https://doi.org/10.1016/j.advwatres.2012.07.010

Allen, R. G., Pereira, L. S., Raes, D., & Smith, M. (1998). *FAO irrigation and drainage paper 56*. Rome.

Baldocchi, D. D., Falge, E., Gu, L., Olson, R., Hollinger, D. Y., Running, S., et al. (2001). FLUXNET: A new tool to study the temporal and spatial variability of ecosystem-scale carbon dioxide, water vapor, and energy flux densities. *Bulletin of the American Meteorological Society*, *82*, 2415–2434. https://doi.org/10.1175/1520-0477(2001)082<2415:FANTTS>2.3.CO;2

Baldocchi, D. D., & Wilson, K. B. (2001). Modeling CO_2 and water vapor exchange of a temperate broadleaved forest across hourly to decadal time scales. *Ecological Modelling*, *142*(1–2), 155–184. https://doi.org/10.1016/S0304-3800(01)00287-3

Barbeta, A., Ogaya, R., & Penuelas, J. (2012). Comparative study of diurnal and nocturnal sap flow of Quercus ilex and Phillyrea latifolia in a Mediterranean holm oak forest in Prades (Catalonia, NE Spain). *Trees - Structure and Function*, *26*(5), 1651–1659. https://doi.org/10.1007/s00468-012-0741-4

Barbour, M. M., & Buckley, T. N. (2007). The stomatal response to evaporative demand persists at night in Ricinus communis plants with high nocturnal conductance. *Plant, Cell and Environment*, *30*(6), 711–721. https://doi.org/10.1111/j.1365-3040.2007.01658.x

Beringer, J., Hutley, L. B., McHugh, I., Arndt, S. K., Campbell, D., Cleugh, H. A., et al. (2016). An introduction to the Australian and New Zealand flux tower network-OzFlux. *Biogeosciences*, *13*, 5895–5916. https://doi.org/10.5194/bg-13-5895-2016

Berkelhammer, M., Hu, J., Bailey, A., Noone, D., Still, C. J., Barnard, H. R., et al. (2013). The nocturnal water cycle in an open-canopy forest. *Journal of Geophysical Research*, *118*(17), 10225–10242. https://doi.org/10.1002/jgrd.50701

Breiman, L., Friedman, J. H., Olshen, R. A., & Stone, C. J. (1984). *Classification and regression tree*. Belmont, CA: Wadsworth International Group.

Bucci, S. J., Scholz, F. G., Goldstein, G., Meinzer, F. C., Hinojosa, J. A., Hoffmann, W. A., et al. (2004). Processes preventing nocturnal equilibration between leaf and soil water potential in tropical savanna woody species. *Tree Physiology*, *24*(10), 1119–1127. https://doi.org/10.1093/treephys/24.10.1119

Cavenderbares, J., Sack, L., & Savage, J. A. (2007). Atmospheric and soil drought reduce nocturnal conductance in live oaks. *Tree Physiology*, *27*(4), 611–620. https://doi.org/10.1093/treephys/27.4.611

Chaves, M. M., Costa, J. M., Zarrouk, O., Pinheiro, C., Lopes, C. M., & Pereira, J. S. (2016). Controlling stomatal aperture in semi-arid regions: The dilemma of saving water or being cool? *Plant Science*, *251*, 54–64. https://doi.org/10.1016/j.plantsci.2016.06.015

Chen, J., Jönsson, P., Tamura, M., Gu, Z., Matsushita, B., & Eklundh, L. (2004). A simple method for reconstructing a high quality NDVI time-series data set based on the Savitzky-Golay filter. *Remote Sensing of Environment*, *91*, 332–344. https://doi.org/10.1016/j.rse.2004.03.014

Dawson, T. E., Burgess, S. S., Tu, K. P., Oliveira, R. S., Santiago, L. S., Fisher, J. B., et al. (2007). Nighttime transpiration in woody plants from contrasting ecosystems. *Tree Physiology*, *27*, 561–575. https://doi.org/10.1093/treephys/27.4.561

Dilshad, M., Motha, J., & Peel, L. (1996). Surface runoff, soil and nutrient losses from farming systems in the Australian semi-arid tropics. *Australian Journal of Experimental Agriculture*, *36*(8), 1003–1012. https://doi.org/10.1071/ea9961003

Domec, J. C., Ogée, J., Noormets, A., Jouangy, J., Gavazzi, M., Treasure, E., et al. (2012). Interactive effects of nocturnal transpiration and climate change on the root hydraulic redistribution and carbon and water budgets of southern United States pine plantations. *Tree Physiology*, *32*(6), 707–723. https://doi.org/10.1093/treephys/tps018

Dormann, C. F., Elith, J., Bacher, S., Buchmann, C., Carl, G., Carré, G., et al. (2013). Collinearity: A review of methods to deal with it and a simulation study evaluating their performance. *Ecography*, *36*(1), 27–46. https://doi.org/10.1111/j.1600-0587.2012.07348.x

Duursma, R. A., Blackman, C. J., Lopéz, R., Martin-StPaul, K., Cochard, H., & Medlyn, B. E. (2019). On the minimum leaf conductance: Its role in models of plant water use, and ecological and environmental controls. *New Phytologist*, *221*(2), 693–705. https://doi.org/10.1111/nph.15395

Elith, J., Leathwick, J. R., & Hastie, T. (2008). A working guide to boosted regression trees. *Journal of Animal Ecology*, *77*(4), 802–813. https://doi.org/10.1111/j.1365-2656.2008.01390.x

Falge, E., Baldocchi, D., OlsonAnthoni, R. P., Aubinet, M., Bernhofer, C., et al. (2001). Gap filling strategies for long term energy flux data sets. *Agricultural and Forest Meteorology*, *107*(1), 71–77. https://doi.org/10.1016/S0168-1923(00)00235-5

Fatichi, S., & Ivanov, V. Y. (2014). Interannual variability of evapotranspiration and vegetation productivity. *Water Resources Research*, *50*(4), 3275–3294. https://doi.org/10.1002/2013WR015044

Fisher, J. B., Melton, F., Middleton, E. M., Hain, C. R., Anderson, M. C., Allen, R. G., et al. (2017). The future of evapotranspiration: Global requirements for ecosystem functioning, carbon and climate feedbacks, agricultural management, and water resources. *Water Resources Research*, *53*(4), 2618–2626. https://doi.org/10.1002/2016WR020175

Forster, M. A. (2014). How significant is nocturnal sap flow? *Tree Physiology*, *34*(7), 757–765. https://doi.org/10.1093/treephys/tpu051

Green, S., Mcnaughton, K. G., & Clothier, B. E. (1989). Observations of night-time water use in kiwifruit vines and apple trees. *Agricultural and Forest Meteorology*, *48*(3), 251–261. https://doi.org/10.1016/0168-1923(89)90072-5

Groh, J., Pütz, T., Gerke, H., Vanderborght, J., & Vereecken, H. (2019). Quantification and prediction of nighttime evapotranspiration for two distinct grassland ecosystems. *Water Resources Research*, *55*(4), 2961–2975. https://doi.org/10.1029/2018WR024072

Gu, L., Meyers, T., Pallardy, S. G., Hanson, P. J., Bai, Y., Heuer, M., et al. (2006). Direct and indirect effects of atmospheric conditions and soil moisture on surface energy partitioning revealed by a prolonged drought at a temperate forest site. *Journal of Geophysical Research*, *111*, D16102. https://doi.org/10.1029/2006JD007161

Haghighi, E., Short Gianotti, D. J., Akbar, R., Salvucci, G. D., & Entekhabi, D. (2018). Soil and atmospheric controls on the land surface energy balance: A generalized framework for distinguishing moisture-limited and energy-limited evaporation regimes. *Water Resources Research*, *54*, 1831–1851. https://doi.org/10.1002/2017WR021729

Han, Q., Liu, Q., Wang, T., Wang, L., Di, C., Chen, X., et al. (2020). Diagnosis of environmental controls on daily actual evapotranspiration across a global flux tower network: The roles of water and energy. *Environmental Research Letters*, *15*, 124070. https://doi.org/10.1088/1748-9326/abcc8c

Horn, J., & Schulz, K. (2010). Post-processing analysis of MODIS leaf area index subsets. *Journal of Applied Remote Sensing*, *4*(1), 043557. https://doi.org/10.1117/1.3524265

Huang, Y., Guo, H., Chen, X., Chen, Z., van der Tol, C., Zhou, Y., et al. (2019). Meteorological controls on evapotranspiration over a coastal salt marsh ecosystem under tidal influence. *Agricultural and Forest Meteorology*, *279*, 107755. https://doi.org/10.1016/j.agrformet.2019.107755

Hutley, L. B., Beringer, J., Isaac, P., Hacker, J. M., & Cernusak, L. A. (2011). A sub-continental scale living laboratory: Spatial patterns of savanna vegetation over a rainfall gradient in northern Australia. *Agricultural and Forest Meteorology*, *151*(11), 1417–1428. https://doi.org/10.1016/j.agrformet.2011.03.002

Iritz, Z., & Lindroth, A. (1994). Night-time evaporation from a short-rotation willow stand. *Journal of Hydrology*, *157*, 235–245. https://doi.org/10.1016/0022-1694(94)90107-4

Isbell, R. F. (2002). *The Australian soil classification*. Melbourne, Australia: CSIRO Publishing.

Jacobs, A. F. G., Heusinkveld, B. G., Kruit, R. J. W., & Berkowicz, S. M. (2006). Contribution of dew to the water budget of a grassland area in the Netherlands. *Water Resources Research*, *42*(3), 446–455. https://doi.org/10.1029/2005WR004055

Jolly, P. (2002). Water balance for the daly river catchment, northern territory, Australia. *Balancing the groundwater budget conference, Darwin, 12–17 May 2002*. Paper. Published on CD-Rom.

Karpul, R. H., & West, A. G. (2016). Wind drives nocturnal, but not diurnal, transpiration in *Leucospermum conocarpodendron* trees: Implications for stilling on the Cape Peninsula. *Tree Physiology*, *36*(8), 954–966. https://doi.org/10.1093/treephys/tpw033

Katul, G. G., Oren, R., Manzoni, S., Higgins, C. W., & Parlange, M. B. (2012). Evapotranspiration: A process driving mass transport and energy exchange in the soil-plant-atmosphere-climate system. *Reviews of Geophysics*, *50*, RG3002. https://doi.org/10.1029/2011RG000366

Leuning, R. (1995). A critical-appraisal of a combined stomatal-photosynthesis model for c-3 plants. *Plant, Cell and Environment*, *18*(4), 339–355. https://doi.org/10.1111/j.1365-3040.1995.tb00370.x

Liu, L., Gudmundsson, L., Hauser, M., Qin, D., Li, S., & Seneviratne, S. I. (2020). Soil moisture dominates dryness stress on ecosystem production globally. *Nature Communications*, *11*(1), 4892. https://doi.org/10.1038/s41467-020-18631-1

Liu, Q., Wang, T., Han, Q., Sun, S., Liu, C.-q., & Chen, X. (2019). Diagnosing environmental controls on actual evapotranspiration and evaporative fraction in a water-limited region from northwest China. *Journal of Hydrology*, *578*, 124045. https://doi.org/10.1016/j.jhydrol.2019.124045

Liu, X., Li, Y., Chen, X., Zhou, G., Cheng, J., Zhang, D., et al. (2015). Partitioning evapotranspiration in an intact forested watershed in southern China. *Ecohydrology*, *8*(6), 1037–1047. https://doi.org/10.1002/eco.1561

Lombardozzi, D., Zeppel, M. J. B., Fisher, R. A., & Tawfik, A. B. (2017). Representing nighttime and minimum conductance in CLM4.5: Global hydrology and carbon sensitivity analysis using observational constraints. *Geoscientific Model Development*, *10*(1), 321–331. https://doi.org/10.5194/gmd-10-321-2017

Malek, E. (1992). Night-time evapotranspiration vs. daytime and 24 h evapotranspiration. *Journal of Hydrology*, *138*(1–2), 119–129. https://doi.org/10.1016/0022-1694(92)90159-S

Meinzer, F. C., Goldstein, G., Jackson, P. C., Holbrook, N. M., Gutierrez, M. V., & Cavelier, J. (1995). Environmental and physiological regulation of transpiration in tropical forest gap species: The influence of boundary layer and hydraulic properties. *Oecologia*, *101*(4), 514–522. https://doi.org/10.1007/BF00329432

Milly, P. C. D., & Dunne, K. A. (2002). Macroscale water fluxes 2. Water and energy supply control of their interannual variability. *Water Resources Research*, *38*(10), 1206. https://doi.org/10.1029/2001WR000760

Moffat, A. M., Papale, D., Reichstein, M., Hollinger, D. Y., Richardson, A. D., Barr, A. G., et al. (2007). Comprehensive comparison of gap-filling techniques for eddy covariance net carbon fluxes. *Agricultural and Forest Meteorology*, *147*(3–4), 209–232. https://doi.org/10.1016/j.agrformet.2007.08.011

Moore, G. W., Cleverly, J., & Owens, M. K. (2008). Nocturnal transpiration in riparian Tamarix thickets authenticated by sap flux, eddy covariance and leaf gas exchange measurements. *Tree Physiology*, *28*(4), 521–528. https://doi.org/10.1093/treephys/28.4.521

Moro, M. J., Were, A., Villagarcía, L., Cantón, Y., & Domingo, F. (2007). Dew measurement by Eddy covariance and wetness sensor in a semiarid ecosystem of SE Spain. *Journal of Hydrology*, *335*(3–4), 295–302. https://doi.org/10.1016/j.jhydrol.2006.11.019

Novick, K. A., Ficklin, D. L., Stoy, P. C., Williams, C. A., Bohrer, G., Oishi, A. C., et al. (2016). The increasing importance of atmospheric demand for ecosystem water and carbon fluxes. *Nature Climate Change*, *6*(11), 1023–1027. https://doi.org/10.1038/nclimate3114

Novick, K. A., Oren, R., Stoy, P. C., Siqueira, M., & Katul, G. G. (2009). Nocturnal evapotranspiration in eddy-covariance records from three co-located ecosystems in the Southeastern US: Implications for annual fluxes. *Agricultural and Forest Meteorology*, *149*(9), 1491–1504. https://doi.org/10.1016/j.agrformet.2009.04.005

Ogée, J., Brunet, Y., Loustau, D., Berbigier, P., & Delzon, S. (2003). MuSICA, a CO_2, water and energy multi-layer, multi-leaf pine forest model: Evaluation from hourly to yearly time scales and sensitivity analysis. *Global Change Biology*, *9*(5), 697–717. https://doi.org/10.1046/j.1365-2486.2003.00628.x

Ogle, K., Lucas, R. W., Bentley, L. P., Cable, J. M., Barron-Gafford, G. A., Griffith, A., et al. (2012). Differential daytime and night-time stomatal behavior in plants from North American deserts. *New Phytologist*, *194*(2), 464–476. https://doi.org/10.1111/j.1469-8137.2012.04068.x

O'keefe, K., & Nippert, J. B. (2018). Drivers of nocturnal water flux in a tallgrass prairie. *Functional Ecology*, *32*(5), 1155–1167. https://doi.org/10.1111/1365-2435.13072

Padrón, R. S., Gudmundsson, L., Michel, D., & Seneviratne, S. I. (2020). Terrestrial water loss at night: Global relevance from observations and climate models. *Hydrology and Earth System Sciences*, *24*(2), 793–807. https://doi.org/10.5194/hess-24-793-2020

Pastorello, G., Trotta, C., Canfora, E., Chu, H., Christianson, D., Cheah, Y. W., et al. (2020). The FLUXNET2015 dataset and the ONEFlux processing pipeline for eddy covariance data. *Scientific Data*, *7*(1), 225. https://doi.org/10.1038/s41597-020-0534-3

Phillips, N. G., Lewis, J. D., Logan, B. A., & Tissue, D. T. (2010). Inter- and intra-specific variation in nocturnal water transport in *Eucalyptus*. *Tree Physiology*, *30*(5), 586–596. https://doi.org/10.1093/treephys/tpq009

R Core Team. (2018). *R software (version 3.5.1)*. Retrieved from https://cran.r-project.org/bin/windows/base/old/3.5.1/

Reichstein, M., Falge, E., Baldocchi, D., Papale, D., & Valentini, R. (2005). On the Separation of Net Ecosystem Exchange into Assimilation and Ecosystem Respiration: Review and Improved Algorithm. *Global Change Biology*, *11*(9), 1424–1439. https://doi.org/10.1111/j.1365-2486.2005.001002.x

Resco De Dios, V., Roy, J., Ferrio, J. P., Alday, J. G., Landais, D., Milcu, A., et al. (2015). Processes driving nocturnal transpiration and implications for estimating land evapotranspiration. *Scientific Reports*, *5*(1), 10975. https://doi.org/10.1038/srep10975

Schulze, E. D., Williams, R. J., Farquhar, G. D., Schulze, W. X., Langridge, J., Miller, J. M., et al. (1998). Carbon and nitrogen isotope discrimination and nitrogen nutrition of trees along a rainfall gradient in northern Australia. *Australian Journal of Plant Physiology*, *25*(4), 413–425. https://doi.org/10.1071/pp97113

Scott, R. L., & Biederman, J. A. (2019). Critical zone water balance over 13 years in a semiarid savanna. *Water Resources Research*, *55*(1), 574–588. https://doi.org/10.1029/2018WR023477

Shangguan, W., Dai, Y., Duan, Q., Liu, B., & Yuan, H. (2014). A global soil data set for earth system modeling. *Journal of Advances in Modeling Earth Systems*, *6*(1), 249–263. https://doi.org/10.1002/2013MS000293

Skaggs, K. E., & Irmak, S. (2011). Characterization of nighttime evapotranspiration and other surface energy fluxes and interactions with microclimatic variables in subsurface drip and center-pivot irrigated soybean fields. *Transactions of the ASABE*, *54*(3), 941–952. https://doi.org/10.13031/2013.37119

Song, X., Lyu, S., & Wen, X. (2020). Limitation of soil moisture on the response of transpiration to vapor pressure deficit in a subtropical coniferous plantation subjected to seasonal drought. *Journal of Hydrology*, *591*, 125301. https://doi.org/10.1016/j.jhydrol.2020.125301

Stoy, P. C., Mauder, M., Foken, T., Marcolla, B., Boegh, E., Ibrom, A., et al. (2013). A data-driven analysis of energy balance closure across FLUXNET research sites: The role of landscape scale heterogeneity. *Agricultural and Forest Meteorology*, *171–172*(3), 137–152. https://doi.org/10.1016/j.agrformet.2012.11.004

Sulman, B. N., Roman, D. T., Yi, K., Wang, L., Phillips, R. P., & Novick, K. A. (2016). High atmospheric demand for water can limit forest carbon uptake and transpiration as severely as dry soil. *Geophysical Research Letters*, *43*(18), 9686–9695. https://doi.org/10.1002/2016GL069416

Tolk, J. A., Howell, T. A., & Evett, S. R. (2006). Nighttime Evapotranspiration from Alfalfa and Cotton in a Semiarid Climate. *Agronomy Journal*, *98*(3), 730–736. https://doi.org/10.2134/agronj2005.0276

Tsuruta, K., Kosugi, Y., Takanashi, S., & Tani, M. (2016). Inter-annual variations and factors controlling evapotranspiration in a temperate Japanese cypress forest. *Hydrological Processes*, *30*(26), 5012–5026. https://doi.org/10.1002/hyp.10977

Vivoni, E. R., Moreno, H. A., Mascaro, G., Rodriguez, J. C., Watts, C. J., Garatuza-Payan, J., et al. (2008). Observed relation between evapotranspiration and soil water in the North American monsoon region. *Geophysical Research Letters*, *35*(22), L22403. https://doi.org/10.1029/2008GL036001

Vuichard, N., & Papale, D. (2015). Filling the gaps in meteorological continuous data measured at FLUXNET sites with ERA-Interim reanalysis. *Earth System Science Data*, *7*(2), 157–171. https://doi.org/10.5194/essd-7-157-2015

Wang, K., & Dickinson, R. E. (2012). A review of global terrestrial evapotranspiration: Observation, modeling, climatology, and climatic variability. *Reviews of Geophysics*, *50*(2), RG2005. https://doi.org/10.1029/2011RG000373

Whitley, R., Beringer, J., Hutley, L. B., Abramowitz, G., De Kauwe, M. G., Duursma, R., et al. (2016). A model inter-comparison study to examine limiting factors in modelling Australian tropical savannas. *Biogeosciences*, *13*(11), 3245–3265. https://doi.org/10.5194/bg-13-3245-2016

Whitley, R., Taylor, D., Macinnis-Ng, C., Zeppel, M., Yunusa, I., O'Grady, A., et al. (2013). Developing an empirical model of canopy water flux describing the common response of transpiration to solar radiation and VPD across five contrasting woodlands and forests. *Hydrological Processes*, *27*(8), 1133–1146. https://doi.org/10.1002/hyp.9280

Williams, I. N., & Torn, M. S. (2015). Vegetation controls on surface heat flux partitioning, and land-atmosphere coupling. *Geophysical Research Letters*, *42*(21), 9416–9424. https://doi.org/10.1002/2015GL066305

Williams, R. J., Duff, G. A., Bowman, D. M. J. S., & Cook, G. D. (1996). Variation in the composition and structure of tropical savannas as a function of rainfall and soil texture along a large-scale climatic gradient in the Northern Territory, Australia. *Journal of Biogeography*, *23*(6), 747–756. https://doi.org/10.1111/j.1365-2699.1996.tb00036.x

Zeppel, M. J. B., David, T., Daniel, T., Catriona, M. N., & Derek, E. (2010). Rates of nocturnal transpiration in two evergreen temperate woodland species with differing water-use strategies. *Tree Physiology*, *30*(8), 988–1000. https://doi.org/10.1093/treephys/tpq053

Zeppel, M. J. B., Lewis, J. D., Phillips, N. G., & Tissue, D. T. (2014). Consequences of nocturnal water loss: A synthesis of regulating factors and implications for capacitance, embolism and use in models. *Tree Physiology*, *34*(10), 1047–1055. https://doi.org/10.1093/treephys/tpu089

Zhang, Q., Manzoni, S., Katul, G., Porporato, A., & Yang, D. (2014). The hysteretic evapotranspiration: Vapor pressure deficit relation. *Journal of Geophysical Research: Biogeosciences*, *119*(2), 125–140. https://doi.org/10.1002/2013JG002484

Zhou, S., Yu, B., Zhang, Y., Huang, Y., & Wang, G. (2016). Partitioning evapotranspiration based on the concept of underlying water use efficiency. *Water Resources Research*, *52*(2), 1160–1175. https://doi.org/10.1002/2015WR017766

Reference From the Supporting Information

Fisher, J. B., Baldocchi, D. D., Misson, L., Dawson, T. E., & Goldstein, A. H. (2007). What the towers don't see at night: Nocturnal sap flow in trees and shrubs at two AmeriFlux sites in California. *Tree Physiology*, *27*(4), 597–610. https://doi.org/10.1093/treephys/27.4.597